

Two-Loop Effects in Low-Energy Electroweak Measurements

A. Aleksejevs

Grenfell Campus of Memorial University, Corner Brook, Canada

S. Barkanova

Acadia University, Wolfville, Canada

V. Zykunov

Belarussian State University of Transport, Gomel, Belarus

We outline the recent results on the two-loop electroweak contributions to the electron-electron scattering cross sections and asymmetries. Although the two-loop corrections are strongly suppressed relative to the one-loop corrections, they still contribute a few percent to the polarization asymmetry, and even this small contribution cannot be ignored at for ultra-precision experiments such as MOLLER planned at JLab. The NNLO calculation techniques we developed for the electron-electron scattering can be adapted for electron-proton processes, electron-positron collisions, and other low-energy experiments involving leptons.

I. MOTIVATION

There are three major ways to look for new physics beyond the Standard Model (SM): the energy frontier (high-energy colliders), the intensity/precision frontier (intense beams) and the cosmic frontier (underground experiments, ground and space-based telescopes). At the precision frontier, one of the most promising processes is polarized electron-electron (Møller) scattering with parity violation, potentially allowing the indirect detection of hypothetical new physics particles coupling to the SM sector through the kinetic mixing. The first measurement of the Møller scattering cross section was done in 1932 [1], but only the recent improvements in precision allowing to measure the parity-violating left-right asymmetry made Møller scattering a candidate for the new-physics sector detection.

The first observation of parity violation in Møller scattering was made by the E-158 experiment at SLAC [2], which studied Møller scattering of 45- to 48-GeV polarized electrons on the unpolarized electrons in a hydrogen target. Its result at low $Q^2 = 0.026 \text{ GeV}^2$, $A_{PV} = (1.31 \pm 0.14 \text{ (stat.)} \pm 0.10 \text{ (syst.)}) \times 10^{-7}$ [3] allowed one of the most important parameters in the Standard Model - the sine of the Weinberg angle (the weak mixing angle) - to be determined with an accuracy of 0.5% ($\sin^2 \theta_W = 0.2397 \pm 0.0010 \pm 0.0008$ in the $\overline{\text{MS}}$ scheme).

A recently-completed JLab experiment measuring the electron-proton scattering asymmetry, Q_{weak} [4], aims to determine $\sin^2 \theta_W$ with relative precision of 0.3%. The results of Q_{weak} commissioning run, constituting about 4% of the data collected [5], give the left-right asymmetry of $A_{PV} = -279 \pm 35 \text{ (stat.)} \pm 31 \text{ (syst.)}$ ppb, the smallest and most precise asymmetry ever measured in e-p scattering, and lead to the first determination of the weak charge of the proton, $Q_W^p = 0.064 \pm 0.012$, in agreement with the SM prediction of $Q_W^p = 0.0710 \pm 0.0007$. From the theory aspect, the Q_{weak} precision can be improved by the better control of hadronic corrections and accounting for

the NNLO contributions to the electron line discussed in this work. With that, and with the full set of data analyzed, Q_{weak} has potential to place tight constraints on the possible SM extensions. Another PV e-p experiment, P2 proposed for the newly-funded MESA facility at Mainz, aims to determine Q_W^p even more precisely, to 2%.

The next-generation experiment to study e-e scattering, MOLLER (Measurement Of a Lepton Lepton Electroweak Reaction) [6], planned at JLab following the 11 GeV upgrade, will offer a new level of sensitivity and measure the PV asymmetry in the scattering of longitudinally polarized electrons off an unpolarized target to a precision of 0.73 ppb. That would allow a determination of the weak mixing angle with an uncertainty of $\delta_{\sin^2 \theta_W}(\overline{\text{MS}}) = \pm 0.00026 \text{ (stat.)} \pm 0.00013 \text{ (syst.)}$ [7], or about 0.1%, an improvement of a factor of five in fractional precision when compared with the E-158 measurement. At such precision, any inconsistency with the Standard Model will signal new physics, so the MOLLER experiment, building on the concept of indirect probes, can provide access to physics at multi-TeV scales. The experiment will undoubtedly be more challenging than previous parity-violating electron scattering experiments, but the MOLLER collaboration has extensive experience in the similar experiments such as MIT Bates, SLAC E158, JLab G0, HAPPEX, PREX and Q_{weak} . The major advantage of the Møller scattering is that e-e scattering asymmetry is much less affected by the uncertainties in the hadronic corrections than e-p asymmetry, and the gamma-Z box radiative correction to PV elastic e-p scattering calculated at 11 GeV in [8] has an accuracy sufficient to keep the uncertainty from this background within the limits of the MOLLER experiment. The rest of the electroweak radiative corrections (EWC), although extensive, can in principle be controlled at sub-1% level, with the SM predictions carried out with full treatment of one-loop radiative corrections and at least leading two-loop corrections.

It was repeatedly shown in the literature that even one-loop radiative corrections modify the tree-level prediction for the asymmetry quite significantly ([9], [10], [11], [12], [13]), so it is essential to have them under a very firm control. (Please see [14] for a review of the low-energy measurements of the weak mixing angle and additional references.) In [12], we found the total correction calculated specifically for 11 GeV e-e scattering to be close to $\sim 65\%$, with no significant theoretical uncertainties. A much larger theoretical uncertainty in the prediction for the asymmetry will come from the two-loop corrections, so, for the new-generation precision measurements, predictions for its scattering asymmetry must include not only a full treatment of one-loop radiative corrections (NLO) but also leading two-loop corrections (NNLO).

We approach the NNLO EWC in stages, by dividing the corrections to the Born ($\sigma_B \sim |M_0|^2$) cross section into two classes: the Q -part induced by quadratic one-loop amplitudes ($\sigma_Q \sim |M_1|^2$), and the T -part corresponding to the interference of the Born and two-loop diagrams ($\sigma_T \sim 2\text{Re}M_2M_0^+$). The details of our calculations for the quadratic one-loop amplitudes, the Q -part, are shown in [15], where, following the same approach we used for NLO EWC, we performed a tuned step-by-step comparison between different calculation approaches verifying the results obtained by a semi-automatic approach based on FeynArts, FormCalc, LoopTools and Form with the results from the equations derived by hand. As we found in [15], for the MOLLER kinematic conditions, the Q -part of the NNLO EWC can increase the asymmetry by up to 4%, and depends quite significantly on the energy and scattering angles.

In this paper, we discuss a set of contributions corresponding to the interference of the Born and two-loop diagrams (the T -part), including the gauge invariant set of boson self energies and vertices of two-loop amplitude M_2 , and discuss work still to be done in the future.

II. CROSS SECTION AND ASYMMETRY

The cross section of polarized Møller scattering with the Born kinematics:

$$e^-(k_1) + e^-(p_1) \rightarrow e^-(k_2) + e^-(p_2), \quad (1)$$

can be expressed as:

$$\sigma = \frac{\pi^3}{2s} |M_0 + M_1 + M_2|^2 \approx \frac{\pi^3}{2s} (M_0M_0^+ + 2\text{Re}M_1M_0^+ + M_1M_1^+ + 2\text{Re}M_2M_0^+), \quad (2)$$

where $\sigma \equiv d\sigma/d\cos\theta$ and θ is the scattering angle of the detected electron with 4-momentum k_2 in the center-of-mass system of the initial electrons. The 4-momenta of initial (k_1 and p_1) and final (k_2 and p_2) electrons generate a standard set of Mandelstam variables:

$$s = (k_1 + p_1)^2, \quad t = (k_1 - k_2)^2, \quad u = (k_2 - p_1)^2. \quad (3)$$

M_0 is the Born ($\mathcal{O}(\alpha)$) amplitude shown in Fig.1. The amplitudes M_1 (Fig.2) and M_2 (Figs.4-8) correspond to one-loop ($\mathcal{O}(\alpha^2)$) and two-loop ($\mathcal{O}(\alpha^3)$) matrix elements, respectively.

The one-loop amplitude M_1 consists of the boson self-energy (BSE) (Fig.2a), vertex (Ver) (Fig.2b,c) and box diagrams (Fig.2d,e). We use the on-shell renormalization scheme from [16, 17], so there are no contributions from the electron self-energies.

We present the one-loop complex amplitude as the sum of IR and IR-finite parts $M_1 = M_1^\lambda + M_1^f$. The IR-finite part M_1^f can be found in [15] and for the IR part we have:

$$M_1^\lambda = \frac{\alpha}{2\pi} \delta_1^\lambda M_0, \quad \delta_1^\lambda = 4B \log \frac{\lambda}{\sqrt{s}}, \quad (4)$$

where λ is the photon mass and the complex value B can be presented in the following form (see, for example, [18]):

$$B = \log \frac{tu}{m^2s} - 1 - i\pi. \quad (5)$$

Analogously, the two-loop amplitude is the sum $M_2 = M_2^\lambda + M_2^f$, where

$$M_2^\lambda = \frac{\alpha}{2\pi} \delta_1^\lambda M_1^f + \frac{1}{8} \left(\frac{\alpha}{\pi} \right)^2 (\delta_1^\lambda)^2 M_0. \quad (6)$$

Note that the structure of first term in (6) is the same as in (4) in terms of the soft photon factorization.

To cancel the infrared divergences, we split the differential cross sections into λ -dependent (IRD-terms) and λ -independent (infrared-finite) parts:

$$\sigma_1 = \sigma_1^\lambda + \sigma_1^f, \quad \sigma_{Q,T}^V = \sigma_{Q,T}^\lambda + \sigma_{Q,T}^f. \quad (7)$$

The one-loop cross section is already carefully evaluated with full control of the uncertainties in [12]. The simplest form for IRD-terms are:

$$\begin{aligned} \sigma_1^\lambda &= \frac{\alpha}{\pi} \text{Re}(\delta_1^\lambda) \sigma_0, \\ \sigma_Q^\lambda &= \left(\frac{\alpha}{2\pi} \right)^2 \left[|\delta_1^\lambda|^2 + 2\text{Re}(\delta_1^f \delta_1^{\lambda*}) \right] \sigma^0, \\ \sigma_T^\lambda &= \left(\frac{\alpha}{2\pi} \right)^2 \text{Re} \left[(\delta_1^\lambda)^2 + 2(\delta_1^f \delta_1^\lambda) \right] \sigma^0. \end{aligned} \quad (8)$$

The imaginary part of the total cross section could be removed in the sum Q - and T -parts due to following properties: $|\delta_1^\lambda|^2 + \text{Re}(\delta_1^\lambda)^2 = 2(\text{Re} \delta_1^\lambda)^2$, and $\text{Re}(\delta_1^f \delta_1^{\lambda*}) + \text{Re}(\delta_1^f \delta_1^\lambda) = \text{Re}(\delta_1^f) \text{Re}(\delta_1^\lambda)$. Thus, in the following sections we can ignore the imaginary part, i. e. $\delta_1^\lambda \rightarrow \text{Re} \delta_1^\lambda$ and $B \rightarrow \text{Re} B$.

III. BREMSSTRAHLUNG FOR NLO AND NNLO

Bremsstrahlung for both NLO (Fig.3a) and NNLO (Fig.3b,c) is needed to cancel the infrared divergences in

the one-loop and two-loop amplitudes, correspondingly. (Radiation from only one lepton line is shown in Fig.3, but all four lepton lines are accounted for in our calculations, of course.) To evaluate the cross section induced by the emission of one soft photon with energy less than ω , we follow the methods of [19] (see also [20]). Then, this cross section can be expressed as: $\sigma^\gamma = \sigma_1^\gamma + \sigma_2^\gamma$, where $\sigma_{1,2}^\gamma$ have the similar factorized structure based on the factorization of the soft-photon bremsstrahlung:

$$\sigma_{1,2}^\gamma = \frac{\alpha}{\pi} [-\delta_1^\lambda + R_1] \sigma_{0,1}, \quad (9)$$

where

$$R_1 = -4B \log \frac{\sqrt{s}}{2\omega} - \left(\log \frac{s}{m^2} - 1 \right)^2 + 1 - \frac{\pi^2}{3} + \log^2 \frac{u}{t}. \quad (10)$$

The first part of the soft-photon cross section, σ_1^γ , cancels the IRD at the one-loop order, while the second part, σ_2^γ , cancels the IRD at the two-loop order, with half of σ_2^γ going to the cancellation of the IRD in the Q -part and the other half going to treat IRD in the T -part. At last, the cross section induced by the emission of two soft photons with a total energy less than ω is calculated in [15] as:

$$\sigma^{\gamma\gamma} = \frac{1}{2} \left(\frac{\alpha}{\pi} \right)^2 ((-\delta_1^\lambda + R_1)^2 - R_2) \sigma_0, \quad (11)$$

where $\frac{1}{2}$ is a statistical factor and $R_2 = \frac{8}{3} \pi^2 B^2$.

Bringing all terms together, we arrive at the result that is free from infrared divergences. For one loop, the logarithms will cancel out:

$$\sigma_{\text{NLO}} = \sigma_1 + \sigma_1^\gamma = \frac{\alpha}{\pi} [R_1 + \delta_1^f] \sigma^0. \quad (12)$$

For the second loop, the cancellation proceeds in a more involved way, that is

$$\begin{aligned} \sigma_{\text{NNLO}} &= \sigma_Q^V + \sigma_T^V + \sigma_2^\gamma + \sigma^{\gamma\gamma} \\ &= \left(\frac{\alpha}{\pi} \right)^2 [R_1 \delta_1^f + \frac{1}{2} R_1^2 - \frac{1}{2} R_2 + \delta_Q^f + \delta_T^f] \sigma^0 \\ &= \sigma_O^f + \sigma_B^f + \sigma_Q^f + \sigma_T^f, \end{aligned} \quad (13)$$

where

$$\sigma_O^f = \frac{\alpha}{\pi} R_1 \sigma_{\text{NLO}}, \quad \sigma_B^f = -\frac{1}{2} \left(\frac{\alpha}{\pi} \right)^2 (R_1^2 + R_2) \sigma^0. \quad (14)$$

IV. NUMERICAL RESULTS

For the numerical calculations at the central kinematic point of MOLLER ($E_{lab}=11$ GeV, $\theta = \pi/2$) we use α , m_W , m_Z and lepton masses as input parameters in accordance with [21]. The effective quark masses which we use for the vector boson self-energy loop contributions are extracted from shifts in the fine structure constant due to

hadronic vacuum polarization $\Delta\alpha_{had}^{(5)}(m_Z^2)=0.02757$ [22]. For the mass of the Higgs boson, we take $m_H = 125$ GeV and for the maximum soft photon energy we use $\omega = 0.05\sqrt{s}$, according to [12] and [23].

Let us define the relative corrections to the Born cross section due to a specific type of contributions (labeled by C) as

$$\delta^C = (\sigma^C - \sigma^0)/\sigma^0, \quad C = \text{NLO}, O, B, Q, T, \text{NNLO}.$$

In the text below the term " T -part" corresponds to the contributions of a gauge invariant set of the BSE and vertices only. The parity-violating asymmetry is defined in a traditional way:

$$A_{LR} = \frac{\sigma_{LL} - \sigma_{RR}}{\sigma_{LL} + 2\sigma_{LR} + \sigma_{RR}}, \quad (15)$$

and the relative corrections to the Born asymmetry due to C -contribution are defined as

$$\delta_A^C = (A_{LR}^C - A_{LR}^0)/A_{LR}^0.$$

In general, corrections from different diagrams are not additive. Their total contribution is given by

$$\delta_A^{\Sigma C_i} = \frac{\Sigma(1 + \delta^{C_i})\delta_A^{C_i}}{1 + \Sigma\delta^{C_i}}, \quad (16)$$

where summation is performed over the index i . There are reasons to believe that the correction δ^{NNLO} is small, but we can not say the same about δ_A^{NNLO} .

In the table below we bring together all contributions derived for relative corrections to the unpolarized cross section to the asymmetry, including contributions that stem from the gauge-invariant set of two-loop vertex and boson-self-energy diagrams. The three dots mean the contribution from the line above, so we progressively add new contributions as we have them ready. So far, as one can see from the table, the Q -part induced by quadratic one-loop amplitudes ($\sim M_1 M_1^+$), and the contributions to T -part corresponding to the interference of the Born and two-loop diagrams ($\sim 2\text{Re}M_2 M_0^+$) considered here shift the result in the same direction. Under the kinematic conditions of the MOLLER experiment, the asymmetry that takes into account the concerted effect of one- and two-loop contributions decreases by about 62.7%. For comparison, the one-loop contribution yield a value of -69.5%. Clearly, there is still a lot to be done, and no definite conclusion can be made until all contributions are accounted for, but it looks like if no major cancellations are introduced by the remaining two-loop contributions, the NNLO effect on the PV asymmetry may be more significant than previously believed. Thus, it is safe to say even now that the research program for the MOLLER experiment must include evaluation of the full set of two-loop corrections. Although our numerical calculations are done for the MOLLER the kinematic conditions, the analytics will be directly applicable for the

collider experiments, so we assume the NLO and NNLO contributions will be affecting their cross section asymmetry significantly as well, and will need to be evaluated for these measurements in the future.

Type of contribution	δ^e	δ_A^C	Published
NLO	-0.1145	-0.6953	[12]
...+(O+B)/2+Q	-0.1125	-0.6536	[15]
...+(O+B)/2+BBSE +VVer+VerBSE	-0.1201	-0.6420	[25]
...+ double boxes	-0.1201	-0.6534	[24]
...+NNLO QED	-0.1152	-0.6500	
...+SE and Ver in boxes	-0.1152	-0.6503	
...+NNLO EW Ver	under way		

V. CONCLUSION

As one can see from our numerical data, at the MOLLER kinematic conditions, the part of the NNLO EWC we considered in this work can increase the asymmetry by up to $\sim 7\%$. The Q - and T -parts do not cancel each other but, on the contrary, they are adding up to increase the physical PV effect. Clearly, the large size of the investigated parts demands a detailed and consistent consideration of the rest of the T -part, which will be the next task of our group. Since the problem of EWC for the Møller scattering asymmetry is rather involved, a tuned step-by-step comparison between different calculation approaches is essential. To make sure that our calculations are error-free, we control our results by comparing the data obtained from the equations derived by hand with the numerical data obtained with a semi-automatic approach based on FeynArts, FormCalc, LoopTools and Form. These base languages have already been successfully employed in similar projects [12] and [13], so we are highly confident in their reliability.

In the future, we plan to address the remaining two-loop electroweak corrections to match the planned precision of the MOLLER experiment and the possible future experiments at ILC. Clearly, for the electroweak low-energy experiments briefly outlined in this paper and for other potential future measurements, it is absolutely essential for an excellent control of one-loop and good understanding of two-loop effects [14].

In this paper, we outlined motivation and summarized some of our work on the two-loop electroweak radiative corrections involving the SM particles. Even if the LHC continues to agree with the Standard Model up to 14 TeV,

the MOLLER experiment will continue to look for new physics scenarios that could escape LHC detection, like various hidden weak scale scenarios. If the LHC does observe an anomaly, then MOLLER will have enough sensitivity to provide sufficient constraints to distinguish between the possible new physics scenarios (new massive or super-massive Z_0 bosons, for example). To have that kind of sensitivity, the MOLLER aims to measure the PV asymmetry predicted within SM to be about 33 ppb with an overall precision of 0.7 ppb. The advantage of trying to access new physics via such low-energy e-e scattering asymmetry is that a purely leptonic PV asymmetry is one of the few observables whose theoretical uncertainties are well under control. There is no significant contribution from the hadronic sector, the SM Higgs mass, one of our input parameters, is known well enough for our needs, and the full set of NLO (one-loop) electroweak radiative corrections, although large, is now known to better than 0.1%. Just a decade ago, such precision would not be feasible. Now, with the recent development in computer algebra and increased accessibility of computing facilities, we can aim to further improve the SM prediction for PV asymmetry by calculating the radiative corrections at the NNLO (two-loop) level. Since the EWC corrections depend quite significantly on the energy and scattering angles, they would need to be evaluated for each experiment specifically. For example, at the MOLLER kinematic conditions, the part of EWC induced by quadratic one-loop amplitudes ($\sim M_1 M_1^+$) will increase the asymmetry up to 4%, but increases dramatically in the higher-energy region [15]. This by itself is not a problem, since the Q -part is now known. However, we still far from making the final conclusion on behavior of the T -part corresponding to the interference of the Born and two-loop diagrams ($\sim 2\text{Re}M_2 M_0^+$). So far, dominant two-loops contributions to the PV asymmetry are at the order of 1% and they are coming from $(\text{Ver} + \text{BSE})^2$ and double boxes. As far as we know at the moment, the new-physics particles are not going to contribute significantly enough at two loops to warrant full-scale calculations, but they may contribute quite noticeably at the one-loop level, depending on the SM extension employed.

VI. ACKNOWLEDGMENTS

The authors gratefully acknowledge Yu. Bystritskiy and E. Kuraev for their help with this project, and the the Joint Institute for Nuclear Research for hospitality in 2013. This work is supported by the Natural Sciences and Engineering Research Council of Canada and Belarus scientific program "Convergence". AA and SB thank JLab Theory Group for hospitality during their stay in 2014.

[1] C. Møller, Ann. der Physik **14**, 531 (1932).

[2] K. S. Kumar *et al.*, Mod. Phys. Lett. A **10**, 2979 (1995);

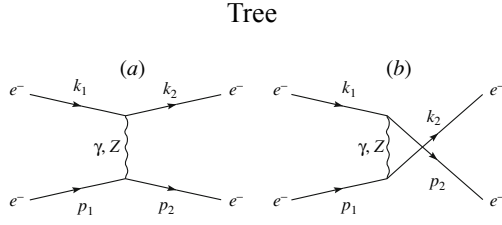


Fig.1 Feynman diagrams corresponding to radiation-free Møller scattering in the (a) t and (b) u channels.

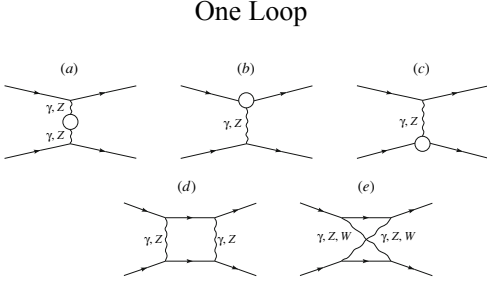


Fig. 2 One-loop t-channel diagrams for the process $e^-e^- \rightarrow e^-e^-$. Here, the circles represent the contributions of self-energies and vertex functions. The respective u-channel diagrams are obtained from those that are presented in this figure by means of the substitutions $k_2 \leftrightarrow p_2$.

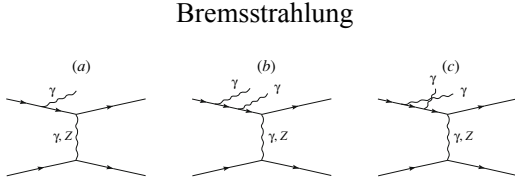


Fig. 3 Diagrams for the processes (a) $e^-e^- \rightarrow e^-e^-\gamma$ and (b, c) $e^-e^- \rightarrow e^-e^-\gamma\gamma$ in the t channel. The u-channel diagrams can be obtained by making the substitutions $k_2 \leftrightarrow p_2$ in the diagrams that are given in this figure. Radiation from only one lepton line is shown.

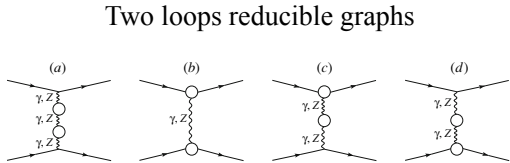


Fig. 4 Two-loop t-channel diagrams from the gauge-invariant set of vertices and boson self-energies. The circles represent the contributions of self-energies and vertex functions. The u-channel diagrams are obtained from those that presented in this figure by means of the substitutions $k_2 \leftrightarrow p_2$.

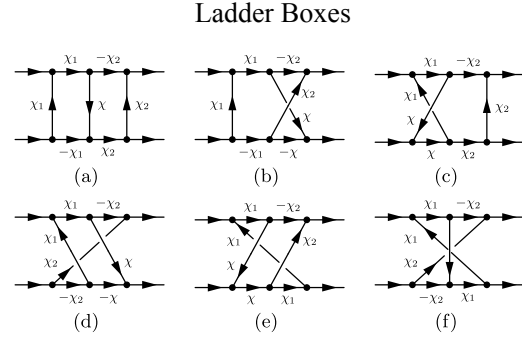


Fig.5 Feynman diagrams topologies corresponding to ladder (double) boxes.

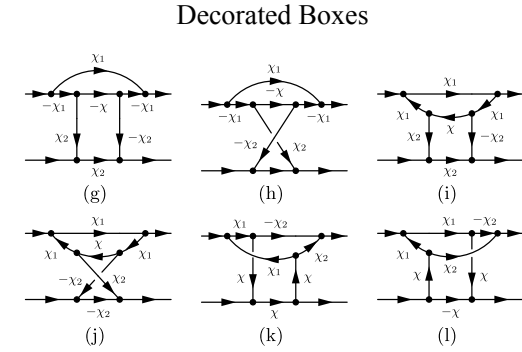


Fig.6 Feynman diagrams topologies corresponding to decorated boxes.

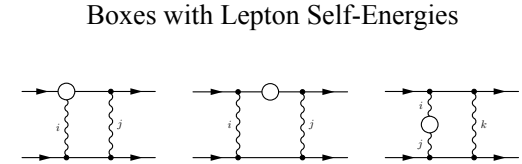


Fig.7 Boxes with vertices (VB), fermion self-energy boxes FSEB and boson self-energy boxes BSEB.

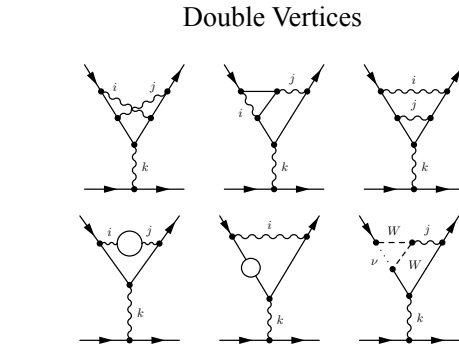


Fig.8 Feynman diagrams with two loops electron vertices.

- Eur. Phys. J. A **32**, 531 (2007); SLAC E158 Collab. P. L. Anthony *et al.*, Phys. Rev. Lett. **92**, 181602 (2004) [hep-ex/0312035].
- [3] P. L. Anthony *et al.*, Phys. Rev. Lett. **95**, 081601 (2005).
- [4] R. D. Carlini *et al.*, Qweak Proposal to Jefferson Lab Program Advisory Committee, arXiv:1202.1255 (2007)
- [5] Qweak Collaboration, Phys.Rev.Lett. **111** (2013) 14, 141803
- [6] The MOLLER Collaboration, "The MOLLER Experiment Measurement Of a Lepton Lepton Electroweak Reaction An Ultra-precise Measurement of the Weak Mixing Angle using Møller Scattering", MIE proposal to US DOE (2014), <http://http://hallaweb.jlab.org/12GeV/Moller/>
- [7] J. Benesch *et al.*, www.jlab.org/~arnd/moller_proposal.pdf (2008)
- [8] N. L. Hall *et al.*, ADP-13-26/T846, JLAB-THY-13-1821, arXiv:1311.3389
- [9] A. Czarnecki and W. J. Marciano, Phys. Rev. D **53**, 1066 (1996) [hep-ph/9507420].
- [10] F. J. Petriello, Phys. Rev. D **67** (2003) 033006, [hep-ph/0210259].
- [11] J. Erler, M. J. Ramsey-Musolf, Phys.Rev. D **72**:073003 (2005)
- [12] A. Aleksejevs *et al.*, Phys. Rev. D **82**, 093013 (2010).
- [13] A. Aleksejevs *et al.*, Phys.Part.Nucl. **44** (2013) 161-174
- [14] K.S. Kumar *et al.*, Ann.Rev.Nucl.Part.Sci. **63** (2013) 237-267
- [15] A. Aleksejevs *et al.*, Phys. Rev. D **85**, 013007 (2012), arXiv:1110.1750 [hep-ph].
- [16] M. Böhm, H. Spiesberger, and W. Hollik, Fortschr. Phys. **34**, 687 (1986).
- [17] A. Denner, Fortsch. Phys. **41**, 307 (1993).
- [18] E. A. Kuraev and V. S. Fadin, Yad. Fiz. **41**, 733 (1985).
- [19] G. 't Hooft and M. Veltman, Nucl. Phys. B. **153**, 365 (1979).
- [20] E. A. Kuraev, N. R. Merenkov, and V. S. Fadin, Yad. Fiz. **45**, 782 (1987).
- [21] C. AMSLER *et al.*, Phys. Lett. B **667**, 1 (2008).
- [22] F. Jegerlehner, J. Phys. G. **29** 101 (2003) [hep-ph/0104304].
- [23] A. Denner and S. Pozzorini, Eur. Phys. J. C **7**, 185 (1999).
- [24] A. Aleksejevs *et al.*, Eur.Phys.J. C **72** (2012) 2249
- [25] A. Aleksejevs *et al.*, Phys.Atom.Nucl. **76** (2013) 888-900, Yad.Fiz. **76** (2013) 942-954